Title

Methylation and phosphorylation of formin homology domain proteins (Fhod1 and Fhod3) by protein arginine methyltransferase 7 (PRMT7) and Rho kinase (ROCK1).

Journal

Journal of Biological Chemistry, 300(11)

Authors

Lowe, Troy
Valencia, Dylan
Velasquez, Vicente
et al.

Publication Date

2024-10-04

DOI

10.1016/j.jbc.2024.107857

Peer reviewed

JBC RESEARCH ARTICLE

Methylation and phosphorylation of formin homology domain proteins (Fhod1 and Fhod3) by protein arginine methyltransferase 7 (PRMT7) and Rho kinase (ROCK1)

Received for publication, April 8, 2024, and in revised form, September 13, 2024 Published, Papers in Press, October 4, 2024,
https://doi.org/10.1016/j.jbc.2024.107857

Troy L. Lowe[1,2], **Dylan A. Valencia**[1,2], **Vicente E. Velasquez**[1], **Margot E. Quinlan**[1,2], **and Steven G. Clarke**[1,2,*]

From the [1]*Department of Chemistry and Biochemistry, University of California, Los Angeles, California, USA;* [2]*Molecular Biology Institute, University of California - Los Angeles, Los Angeles, California, USA*

Reviewed by members of the JBC Editorial Board. Edited by Enrique De La Cruz

Protein post-translational modifications (PTMs) can regulate biological processes by altering an amino acid's bulkiness, charge, and hydrogen bonding interactions. Common modifications include phosphorylation, methylation, acetylation, and ubiquitylation. Although a primary focus of studying PTMs is understanding the effects of a single amino acid modification, the possibility of additional modifications increases the complexity. For example, substrate recognition motifs for arginine methyltransferases and some serine/threonine kinases overlap, leading to potential enzymatic crosstalk. In this study we have shown that the human family of formin homology domain-containing proteins (Fhods) contain a substrate recognition motif specific for human protein arginine methyltransferase 7 (PRMT7). In particular, PRMT7 methylates two arginine residues in the diaphanous autoinhibitory domain (DAD) of the family of Fhod proteins: R1588 and/or R1590 of Fhod3 isoform 4. Additionally, we confirmed that S1589 and S1595 in the DAD domain of Fhod3 can be phosphorylated by Rho/ROCK1 kinase. Significantly, we have determined that if S1589 is phosphorylated then PRMT7 cannot subsequently methylate R1588 or R1590. In contrast, if R1588 or R1590 of Fhod3 is methylated then ROCK1 phosphorylation activity is only slightly affected. Finally, we show that the interaction of the N-terminal DID domain can also inhibit the methylation of the DAD domain. Taken together these results suggest that the family of Fhod proteins, potential *in vivo* substrates for PRMT7, might be regulated by a combination of methylation and phosphorylation.

Protein post-translational modifications enhance biological diversity. Although a generalized consensus of these individual modifications has been proposed, knowledge about the interplay of multiple modifications on biological function is lacking. However, distinct modifications often occur in close proximity on target substrates, creating potential cross-talk in regulatory pathways. Cross-talk may result from binding competition between enzymes or changes in the recognition motif. In particular, histones and transcription factors are known to display a plethora of modifications ultimately leading to the translational regulation of specific genes. For example, the recruitment of TATA-binding proteins (TBPs) and TBP-associated factors (TAFs) to the transcriptional start site of some eukaryotic organisms results in the signaling for polymerase II (1). While phosphorylation is the most dominant modification on TBPs and TAFs (2), additional modifications like acetyllysine (3) and methylarginine (4) are also present.

One modification, protein arginine methylation, is catalyzed by a family of nine enzymes in mammals; whether protein arginine demethylases are involved *in vivo* has not been fully resolved (5, 6). Methylation occurs on the guanidino side chains of arginine residues, increasing the number of potential hydrogen bond donors, increasing the bulk, and altering the distribution of positive charge (7–9). PRMT1-4, 6, and 8 are known as type I PRMTs that catalyze asymmetric dimethylarginine (10), PRMT5 and PRMT9 are considered type II that catalyze symmetric dimethylarginine (11), and PRMT7 is the only type III PRMT exclusively catalyzing monomethylarginine (12). While most of the PRMTs recognize substrates containing arginine and glycine-rich motifs (GARs), PRMT4 prefers proline and glycine motifs, and PRMT7 prefers arginine-x-arginine motifs (RXR) (13, 14).

Protein phosphorylation is catalyzed by kinases and to date there are an estimated 538 protein kinase-encoding genes (15). These protein kinases are classified into eight groups depending on their substrate recognition. In particular, the AKT kinases that phosphorylate serine and threonine residues are known to have a recognition motif sequence of RxRxxS/T and are known to regulate many biological processes including the MAPK pathway and WNT signaling pathway (16). Because PRMT7 and the AKT kinases have overlapping substrate recognition motifs, one might expect some overlap of protein modifications, leading to crosstalk and allosteric regulations. In *Saccharomyces cerevisiae*, proteins Npl3, Ded1, and Sbp1 have been identified to have arginine methylation and phosphorylation co-occuring in regions that are highly disordered (17).

PRMT7 has been implicated in many biological processes including the epithelial to mesenchymal transition in breast cancer (18), the regulation of inflammation through the NF-κ pathway in chronic obstructive pulmonary disease patients

* For correspondence: Steven G. Clarke, clarke@mbi.ucla.edu.

(19), and the maintenance of stem cells during development (20). To date, 51 patients have been documented to have homozygous or compound heterozygous mutations in the PRMT7 gene, leading to a variety of phenotypes due to the presumed absence of enzyme activity (21, 22). These phenotypes are classified as short stature, brachydactyly, intellectual developmental disability, seizures, and hypotonia (23). Additionally, PRMT7 appears to have a major role in skeletal muscle maintenance and formation (24–26).

Actin is one of the most ubiquitous proteins in eukaryotic cells. It is a fundamental element of muscle and plays an important role in cellular architecture and movement (27). Actin nucleators aid in the assembly of actin filaments and are categorized into three classes, Arp2/3 complex, formins, and tandem WASP homology 2 (WH2) nucleators (28). In humans, 15 genes encode the family of formin proteins, and mutations of some of these genes have been linked to cancer, intellectual disability, and developmental defects of the heart (28, 29). All formins contain core formin homology domains unique to the class, FH1 and FH2 (30, 31), and sequence similarity can vary between 20 to 60%, thus creating subclasses. One subfamily of formins, the Formin Homology Domain-containing proteins (Fhods) consists of two proteins in humans, Fhod1 and Fhod3. Fhod1 is highly expressed in many cells, including spleen (32) and skeletal muscle (33). It is found in multiple structures, including stress fibers (34) and transmembrane actin-associated nuclear (TAN) lines (35) that are linked to a range of diseases (29, 36). Fhod3 is mainly expressed in cardiac muscle (37). It is located in the contractile structures, sarcomeres (38, 39), and linked to both dilated and hypertrophic cardiomyopathies (40).

In this article, we show that Fhod1 and Fhod3 proteins are newly identified substrates for PRMT7 and that the phosphorylation of nearby serine residues can inhibit the methylation reactions. Additionally, we observed that methylation of an arginine residue in proximity to a phosphorylatable serine has little effect on ROCK1 kinase.

Results

Human Fhod1 and Fhod3 contain a recognition sequence for PRMT7 similar to human histone H2B

Human histone H2B has been identified as a particularly effective substrate for PRMT7 methylation (14). Specifically, the arginine residues in the RKRSR motif at residues 29 to 33 have been identified as PRMT7 targets and the methylation efficiency of this motif is highly dependent upon its sequence (13). To identify additional proteins that may be substrates for PRMT7, we performed a peptide search for human proteins containing an RKRSR motif (Table S1). Based on the apparent importance of PRMT7 in muscle organization (24–26, 41), we narrowed our search to four proteins classified in the "cytoskeleton organization" gene ontology group (Table 1). Since PRMT7 primarily localizes in the cytoplasm (42, 43), we further focused our attention on the two proteins that were mainly located in the cytoplasm, FH1/FH2 domain-containing proteins 1 and 3.

The C-termini of human Fhod1 and Fhod3 are methylated by human PRMT7

Fhod1 and Fhod3 contain four conserved domains, a diaphanous inhibitory domain (DID), formin homology domains 1 (FH1) and 2 (FH2), and a diaphanous autoregulatory domain (DAD) (Fig. 1*A*). The latter three domains compose the C-terminal half of the protein, with 52% amino acid identity between Fhod1 and Fhod3. The RKRSR motif is present in the DAD region near the C-terminus (Fig. 1*B*). To determine if human Fhod1 and Fhod3 DAD domains can be methylated by PRMT7, we performed *in vitro* methylation assays. We found that the constructs including the DAD domain of MBP-Fhod1 (1110-1164) and Fhod3-CT (963-1162) were, in fact, substrates for PRMT7 (Fig. 1*C*). All further experiments were performed with a shorter fragment of Fhod3, encompassing the tail (MBP-Fhod3-tail (1472-1622)).

There is an additional sequence in the C-terminal domain of Fhod3 (RTRSR) that closely resembles the RKRSR motif of human histone H2B and Fhod1 which may be a methylation site. To determine the localization of PRMT7 methylation site(s), we made mutations in the MBP-Fhod3-tail where we replaced arginine residues with lysine residues to remove the RXR motif. When we mutated the RTRSR motif to RTKSR (R1536K) we found no loss of methylation, suggesting that this site was not a substrate for PRMT7 (Fig. 2). On the other hand, when we mutated the RKRSR motif to KKKSR (R1586/1588K) we found that the protein was no longer a substrate for PRMT7. In this case, we mutated both of the initial arginine residues because the sequence immediately preceding the motif (RE) might have generated an additional RXR sequence. These results provided evidence that the major sites of arginine methylation exclusively reside in the RKRSR sequence within the DAD domain of Fhod3 (Fig. 2).

Arginine residues at positions 1588 and 1590 of HsFhod3 isoform 4 are major methylation sites for PRMT7 catalysis

We next identified the specific arginine residues methylated within the canonical Fhod3 target sequence (RKRSR, 1586-1590). In the histone H2B RKRSR sequence, all three arginine residues were found to be methylated by PRMT7 through the use of mass spectrometry (14). Evidence was presented that the major activity occurred at the first two arginines in the RKRSR motif, R29 and R31 (14). While both Fhod1 and Fhod3 contained the identical RKRSR sequence, an additional RXR motif is present due to the preceding RE residues creating a RERKRSR motif (residues 1584-1590) potentially creating 4 arginines that can be methylated by PRMT7. We mutated each of these arginines in MBP-Fhod3-tail individually to identify which residues are methylated by PRMT7. Upon performing *in vitro* methylation reactions with the MBP-Fhod3-tail R1584K, R1586K, R1588K, and R1590K constructs, we were only able to observe methylation of the R1584K and R1586K constructs, demonstrating that these two residues are not required for methylation and that both R1588 and R1590 are required (Fig. 3). Because R1588 and R1590 straddle a single RXR motif, we interpret these findings as evidence that one or

Table 1
Human cytoskeletal organization proteins containing the specific RKRSR sequence

Accession	Entry name	Protein name	Localization	Gene ontology
O75400	PR40A	Pre-mRNA-processing factor 40 homolog A	Nucleus	Cytoskeleton Organization
P18583	SON	Protein SON	Nucleus	Microtubule Cytoskeleton Organization
Q2V2M9	Fhod3	FH1/FH2 domain-containing protein 3	Cytoplasm	Cortical Actin Cytoskeleton Organization
Q9Y613	Fhod1	FH1/FH2 domain-containing protein 1	Cytoplasm	Cortical Actin Cytoskeleton Organization

both of these positions are the major sites of methylation. Interestingly, in the histone H2B sequence, the first two arginines are preferentially methylated while in the Fhod3 sequence, it is the latter two that are PRMT7 substrates.

Phosphoserine 1589 inhibits methylation by PRMT7, while phosphoserine 1595 only mildly inhibits PRMT7 activity

It has been established that phosphorylation of Fhod3 at serine 1589 by either ROCK1 or ROCK2 kinase regulates the activity of this protein by alleviating its autoinhibition (44, 45). Since we found that the two arginine residues directly adjacent to this serine residue are sites of PRMT7 modification, we asked how the phosphorylation of S1589 impacts the methylation of R1588 and R1590. To do so, we first confirmed that a synthetic peptide containing the recognition motif (Fhod3 residues 1581-1595), is an effective substrate for PRMT7 (Fig. 4*A*). Significantly, we found that phosphorylation of a synthetic peptide containing S1589 resulted in little or no methylation by PRMT7 (Fig. 4*B*). On the other hand, phosphorylation of a downstream serine residue at position 1595 increases the Km four-fold without making a significant change to the Kcat (Fig. 4*C*). These results demonstrate that phosphoserine in close proximity to the RXR PRMT7 substrate recognition site inhibits enzyme activity.

Phosphoserine 32 of human histone H2B inhibits methylation by PRMT7 activity, while phosphoserine 36 mildly inhibits PRMT7 activity

The dramatic inhibition of PRMT7 activity by an adjacent phosphoserine residue seen with the Fhod3 peptide led us to ask if a similar effect is seen with the complementary motif of the H2B peptide. In yeast histone H2B, residues 30 to 37 comprise a repressive domain (46, 47). Additionally, methylatable arginine residues 31 and 33 flank serine 32 which is known to be phosphorylated by RSK2 (48) and by Aurora B kinase (49). Furthermore, the downstream serine 36 residue can be phosphorylated by S6K1 (50) and AMPK (51). While serine 36 is conserved in higher organisms, serine 32 is only

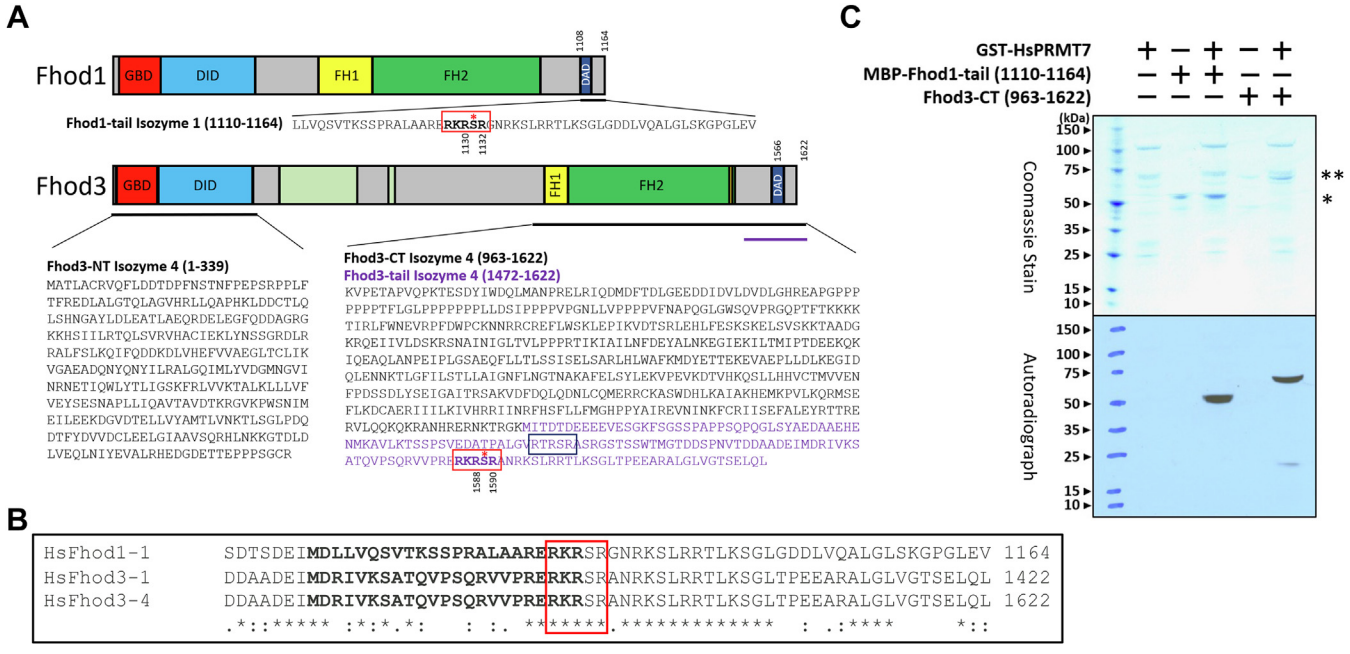

Figure 1. The C-terminal domains of HsFhod1 and HsFhod3 are methylated by HsPRMT7 *in vitro*. *A*, schematic diagram of HsFhod1 and HsFhod3 and constructs used in this paper. Conserved domains are indicated. *Light green boxes* in Fhod3 are inserts that distinguish isozyme 4 from isozyme 1. The *dark blue box* (RTRSR) contains a sequence similar to the PRMT7 recognition sequence (RKRSR), which is in the *red box*. *Red asterisk* (*) denotes a serine that is phosphorylated by ROCK1/2. *B*, sequence alignment of HsFhod1 and HsFhod3 (isozymes 1 and 4) C-terminal residues including the core DAD domain (*bold*) and the PRMT7 recognition motif (*red box*). *C*, 7 μg of MBP-Fhod1-tail or 7 μg of Fhod3-CT, 5 μg of GST-HsPRMT7, and 0.7 μM [^{3}H]AdoMet were combined and allowed to incubate for 20 h at 4 °C in a reaction buffer containing 1 mM DTT, 50 mM K-HEPES, with a final pH of 8.5 in a final volume of 30 μl. Samples were separated by SDS-PAGE electrophoresis and exposed to autoradiography film for 5 days. *Single asterisk* (*) denotes the polypeptide molecular weight of MBP-Fhod1-tail; *double asterisk* (**) denotes the polypeptide molecular weight of Fhod3-CT.

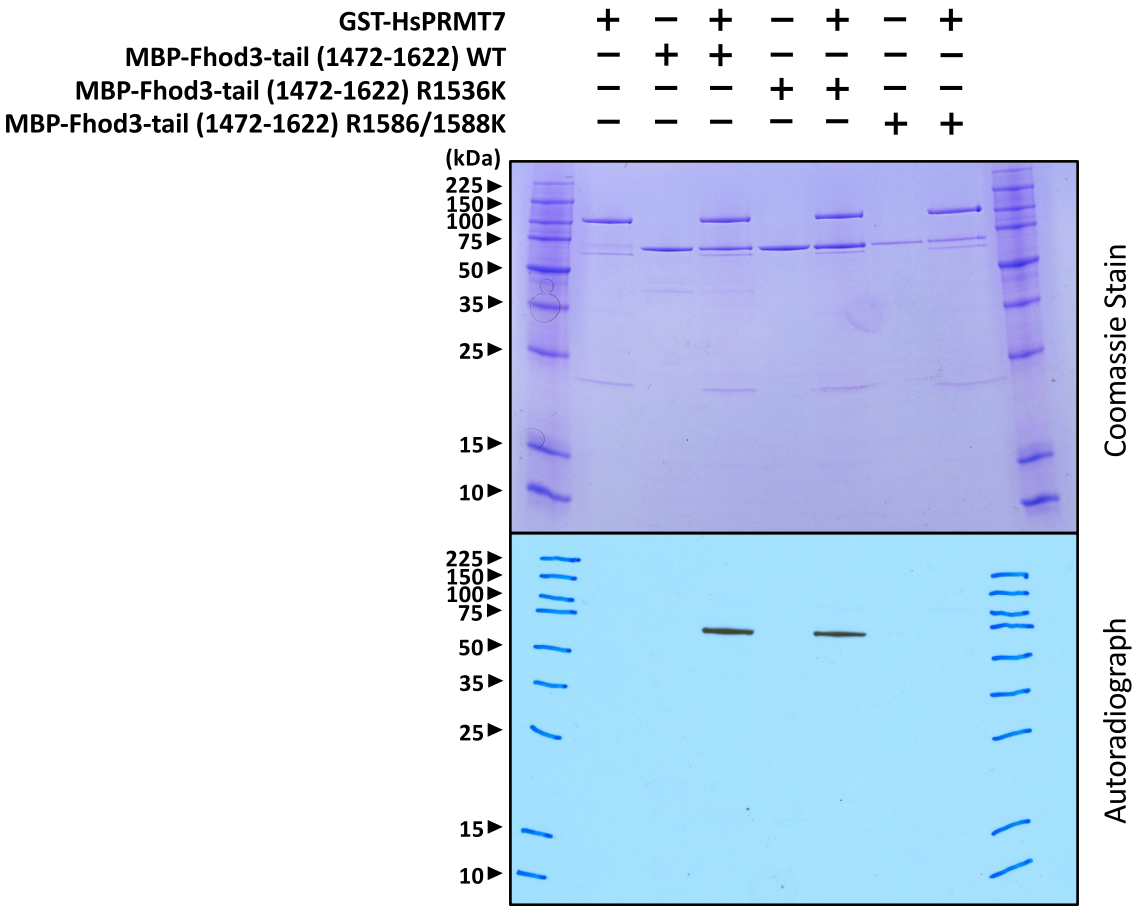

Figure 2. PRMT7 methylates the RKRSR motif of Fhod3 and not the RTRSR motif. 5 μg of GST-HsPRMT7 and 3 μg of MBP-Fhod3-tail constructs were mixed with 0.7 μM [^{3}H]AdoMet in a final volume of 30 μl. Reactions were incubated for 20 h at 4 °C prior to termination by SDS-sample buffer. Samples were separated by SDS-PAGE electrophoresis and exposed to autoradiography film for 10 days. Fhod3 constructs consisted of amino acid residues (1472-1622) from isozyme 4 as the wildtype (WT) sequence or the mutated R1536K sequence or the double mutant R1586K and R1588K sequence. Protein bands at 100 kDa represent GST-HsPRMT7 and protein bands at 63 kDa represent MBP-Fhod3-tail constructs. The total amounts of protein and substrate were determined by nanodrop A280 where 1 μg/μl was equal to 1 absorbance unit.

present in mammals and amphibians (Fig. 5). We first established that *in vitro* methylation with PRMT7 is effective when the substrate is a human histone H2B (23–37) synthetic peptide (Fig. 6). We then performed *in vitro* methylation experiments with peptides containing a phosphoserine at either position 32 or 36. We observed little to no methylation of the H2B (23–37) peptide containing a phosphoserine at position 32 while the peptide containing a phosphoserine at position 36 had a decreased amount of methylation compared to the wild type (Fig. 6). These results demonstrate that inhibition of PRMT7 increases as the phosphoserine gets closer to the arginine recognition sequence in histone H2B, and corroborate the results seen with Fhod3.

Methylarginine 1588 or 1590 minimally affects the phosphorylation of Fhod by ROCK1 in a peptide containing serine 1589 and/or 1595

Since we found that phosphorylation of the serine residue in the RSR methylation motif resulted in the loss of PRMT7 methylation, we then asked whether methylation of these arginine residues affects phosphorylation of the serine residue. Phosphorylation of serine 1589 and 1595 in the RSR motif of the DAD domain of Fhod1/3 by ROCK1/2 is sufficient to relieve autoinhibition, which then activates actin nucleation (44, 45). While the previous ROCK1 phosphorylation studies have been performed both *in vivo* and on truncated C-terminal tail constructs, we first wanted to establish whether ROCK1 could recognize a serine residue in a peptide substrate that we could prepare in methylated and unmethylated forms (45). We thus compared the extent of phosphorylation of Fhod3 peptides containing residues 1581 to 1595 (VVPRERKRSRANRKS) with ROCK1 in *in vitro* time course assays, for up to 2 h, analyzed by LC/MS (Fig. 7). We found clear evidence for phosphorylation of the unmethylated peptide and peptides with a monomethylarginine at either position 1588, or 1590, or both. In contrast to the effect of serine phosphorylation on arginine methylation, we observed no significant decrease in phosphorylation (Fig. 7). These results suggest that methylation of adjacent arginine residues has little effect on ROCK1 phosphorylation.

In the experiment shown in Figure 7, we only detected monophosphorylated peptides even after 2 h of incubation. We then decided to increase the incubation time in hopes of

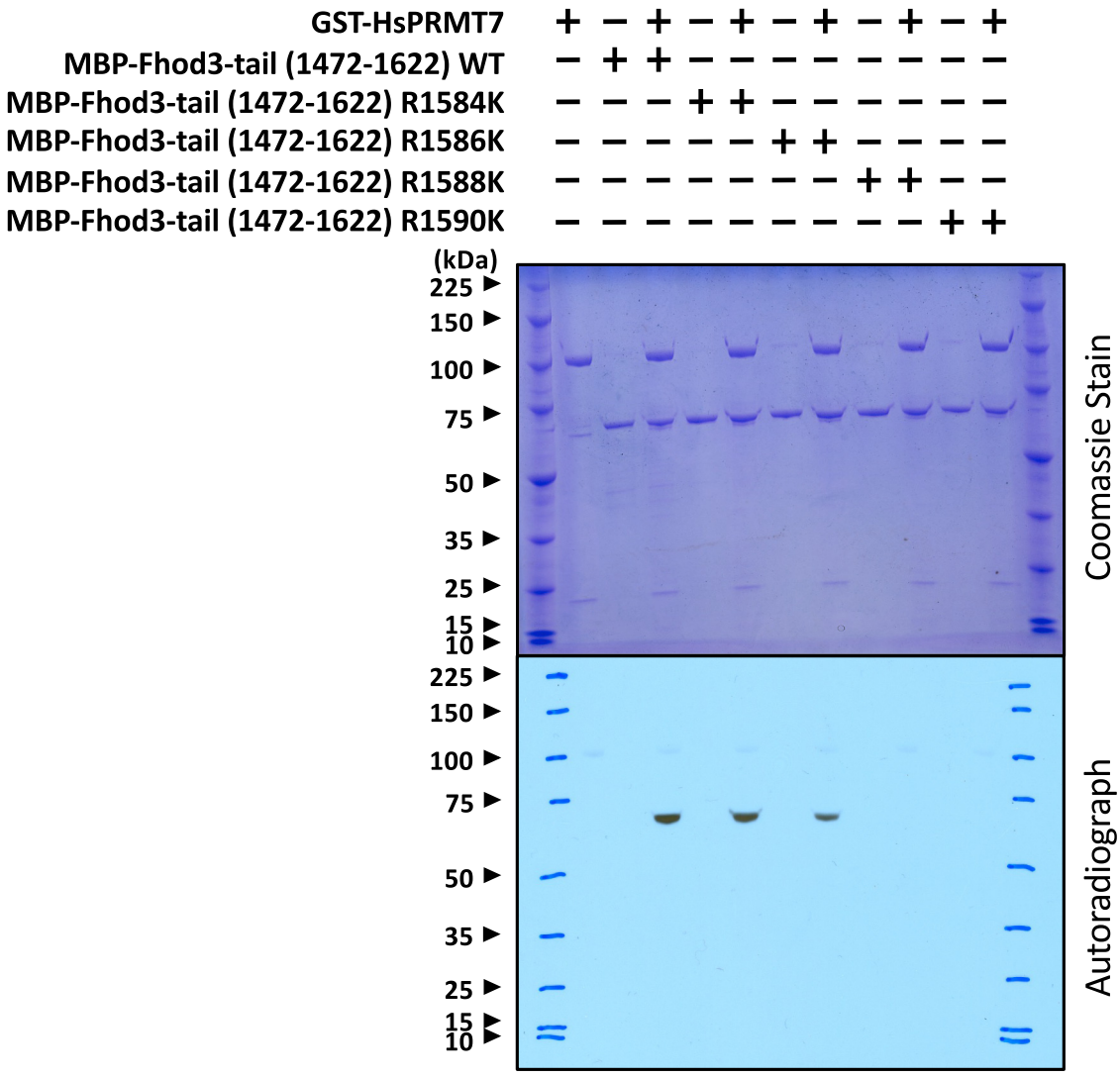

Figure 3. PRMT7 methylates R1588 or R1590 of the Fhod3-tail. 5 μg of GST-HsPRMT7 was mixed with 3 μg of MBP-Fhod3-tail constructs containing mutations of arginine to lysine in the identified RERKRSR motif sequence, and 0.7 μM [^{3}H]AdoMet in a final volume of 30 μl. Reactions were incubated for 20 h at 4 °C and then terminated with an SDS-PAGE sample buffer. Gel was exposed to an autoradiograph film for 10 days prior to development. Total amounts of protein and substrate were determined by nanodrop A280 where 1 μg/μl was equal to 1 absorbance unit.

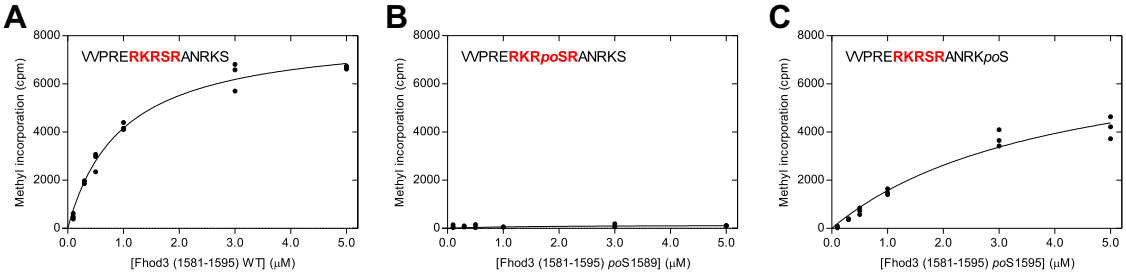

Peptide Name	Peptide Sequence	Km (μM)	Kcat (min^{-1})	Kcat/Km (min^{-1}μM^{-1})
Fhod3 (1581-1595) WT	VVPRERKRSRANRKSY	0.96 ± 0.09	86.7 ± 2.8	90 ± 9
Fhod3 (1581-1595) *po*S1589	VVPRERKR{poS}RANRKSY	1.52 ± 2	1.44 ± 0.82	0.95 ± 1.33
Fhod3 (1581-1595) *po*S1595	VVPRERKRSRANRK{poS}Y	4.06 ± 0.99	84 ± 11	20.8 ± 5.8

Figure 4. Phosphoserine 1589 of Fhod3 inhibits PRMT7 activity. 5 μg of GST-HsPRMT7, 0.14 μM of [^{3}H]AdoMet and indicated Fhod3 (1581-1595) peptides incubated at 20 °C for 1 h in a reaction mixture of 50 mM K-HEPES, 1 mM DTT, and pH of 8.5 in a final volume of 30 μl. *A*, Fhod3 (1581-1595) WT, (*B*) Fhod3 (1581-1595) poS1589, and (*C*) Fhod3 (1581-1595) *po*S1595. Curves were fitted to a standard Michaelis-Menten equation using GraphPad PRISM, n = 3.

	29 31 32 33 36
H. sapiens	KAQKKDGKK**RKRSR**KESYSIYVYK
B. taurus	KAQKKDGKK**RKRSR**KESYSVYVYK
M. musculus	KVQKKDGKK**RKRSR**KESYSVYVYK
X. laevis	KTQKKDGKK**RRKSR**KESYAIYVYK
D. rerio	KTQKKGDKK**RRKTR**KESYAIYVYK
D. melanogaster	NITKT-DKK**KKRKR**KESYAIYIYK
A. thaliana	KEAGDKKKK**RSKKN**VETYKIYIFK
S. cerevisiae	TSTSTDGKK**RSKAR**KETYSSYIYK
H. vulgaris	KIAGTGDKK**RKKKR**RESYAIYIYN

Figure 5. The RKRSR motif of histone H2B is highly conserved among higher order species. The human histone H2B sequence containing PRMT7 recognition residues RKRSR aligned with common model organism histone H2Bs. Higher organisms only contain a serine at position 32. Serine 36 is highly conserved but is altered to threonine in some lower organisms.

capturing a diphosphorylated Fhod3 peptide. In a 5 h incubation, we found that similar amounts of monophosphorylated and diphosphorylated peptides were formed with the unmethylated peptide, the 1588 monomethylated peptide, the 1590 monomethylated peptide, and 1588 and 1590 monomethylated peptide (Figs. S1–S4). These results confirm the general lack of effect of methylation on phosphorylation.

To observe the effect of arginine methylation on the serine residue between the two arginine residues, we designed peptides containing only the Fhod3 sequence 1581-1594 (VVPRERKRSRANRK). In time course experiments with these peptides, containing monomethylarginine residues at positions 1588, 1590, or at 1588 and 1590, we detected monophosphorylation at similar levels as the unmethylated peptide (Fig. 8). Finally, we quantified the ratio of the degree of phosphorylation of the monomethylated peptides to that of the unmodified peptide from the data in Figures 7 and 8. We found that the average ratio for each of the time points for the different charge states varies from 0.41 to 1.77 for the different peptides with an average value of 1.09, confirming that there is no large change in the serine 1589 phosphorylation, catalyzed by ROCK1, of the peptide when arginine residues 1588 and/or 1590 are monomethylated. It is intriguing that phosphorylation has such a powerful negative effect on methylation whereas methylation appears to have a much more limited role on phosphorylation.

The N-terminus of human Fhod3 abolishes methylation of the C-terminus by human PRMT7

Two domains of Fhod3, the DID in the N-terminus and DAD in the C-terminus, come together to form an inhibited protein complex (44, 45). Phosphorylation of Fhod by ROCK1 or ROCK2 kinase is known to alleviate autoinhibition and activate actin assembly (44, 45). To determine if PRMT7 can methylate the C-terminus of Fhod3 in an autoinhibited state we performed *in vitro* methylation reactions with truncated N and C-terminal constructs of Fhod3 (Fhod3-NT (1-339) and MBP-Fhod3-tail). First, we determined that the N-terminus of Fhod3 is itself not methylated by PRMT7 (Fig. 9). Interestingly, we found that Fhod3-NT could inhibit the PRMT7-dependent methylation of the wild-type MBP-Fhod3-tail (Fig. 9). In control experiments, we showed that the Fhod3-NT had no effect on PRMT7 activity itself (Fig. 10). Utilizing a short peptide containing the PRMT7 consensus sequence H2B (23–37), we observed no inhibition of the N-terminus on its

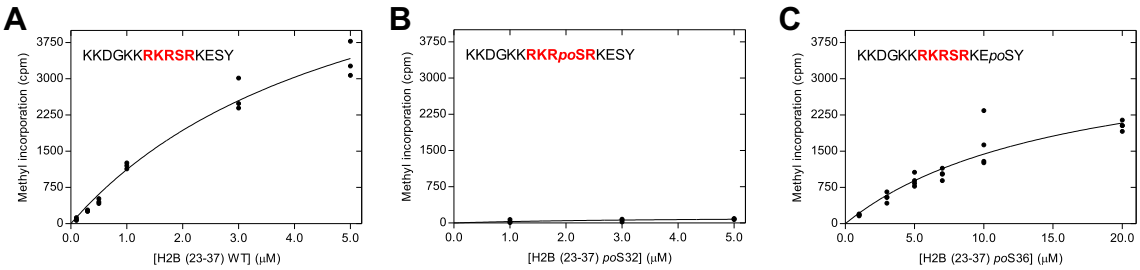

Peptide Name	Peptide Sequence	Km (μM)	Kcat (min^{-1})	Kcat/Km ($min^{-1}μM^{-1}$)
H2B (23-37) WT	Ac-KKDGKKRKRSRKESY-NH_2	5.3 ± 1.3	75 ± 11	14 ± 4
H2B (23-37) *po*S32	KKDGKKRKR{poS}RKESY	3.5 ± 4.7	1.4 ± 0.9	0.4 ± 0.6
H2B (23-37) *po*S36	KKDGKKRKRSRKE{poS}Y	16.2 ± 6.1	40.0 ± 9	2.5 ± 1.1

Figure 6. Phosphoserine 32 of human histone H2B abolishes PRMT7 activity. 5 μg of GST-HsPRMT7 was mixed with either (*A*) H2B (23-37) WT, (*B*) H2B (23-37) *po*S32 or (*C*) H2B (23-37) *po*S36, and 0.7 μM [^{3}H]AdoMet. Reaction mixtures contained 50 mM K-HEPES, 1 mM DTT, pH = 8.5 in a final volume of 30 μl. Reactions were incubated at 20 °C for 1 h prior to termination with 100% TFA. Points were fitted to a standard Michaelis Menten fit equation using GraphPad PRISM, n = 3.

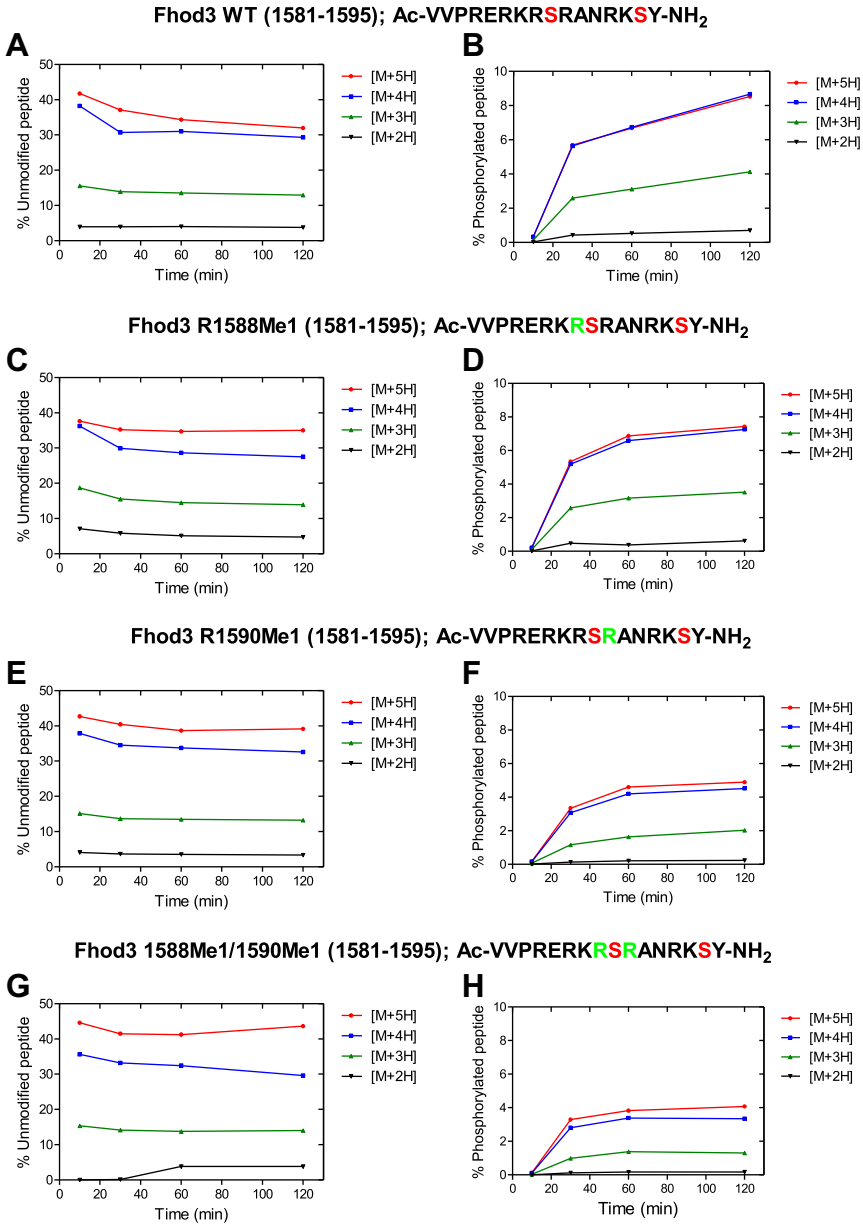

Figure 7. ROCK1 enzymatic activity is minimally affected by the presence of methylarginine residues in a peptide containing serine 1589 and serine 1595. 130 ng of ROCK1, 1 mM ATP and 10 μM Fhod3 (1581-1595) peptides were incubated in a water bath at 30 °C for the specified time in a final volume of 30 μl. Reactions were terminated with TFA and loaded into a vial for mass spectrometry analysis. 10 μl of the sample was injected into an Agilent QTOF 6545 with a run time of 12 min. *A* and *B*, Fhod3 WT, *C* and *D*, Fhod3 R1588Me1, *E* and *F*, Fhod3 R1590Me1, *G* and *H*, Fhod3 R1588Me1/R1590Me1. Change in the total amount of unmodified or phosphorylated peptide in reaction mixtures from charge states [M+2H] (*black line*), [M+3H] (*green line*), [M+4H] (*blue line*), and [M+5H] (*red line*) with time.

methylation (Fig. 10). Additionally, we did not detect inhibition of PRMT7 methyltransferase activity by the Fhod3-NT fragment with the Fhod3 (1581-1595) peptide or with the corresponding *po*S1595, R1588Me1, or R1590Me1 peptides (Fig. 11). These results demonstrate that methylation of the C-terminal tail domain, but not a short peptide containing the methylation site, is inhibited when the Fhod3-NT is present.

Discussion

Previous work has established that PRMT7 can be distinguished from the other members of the mammalian PRMT family both by its specificity for an arginine motif in proteins and by the fact that it is the sole PRMT that catalyzes monomethyl derivatives. This enzyme is characterized by its recognition of certain pairs of arginine residues separated by one residue, the RXR motif (14). A particular variant of this motif found in human histone H2B (RKRSR) has been shown to be an excellent substrate (14). Searching for other proteins containing this motif identified the formin family of proteins as potential substrates.

In this study, we have demonstrated that the DAD domain of the Fhod family of formins can be methylated *in vitro* by PRMT7. Specifically, for Fhod1 and Fhod3, methylation occurs

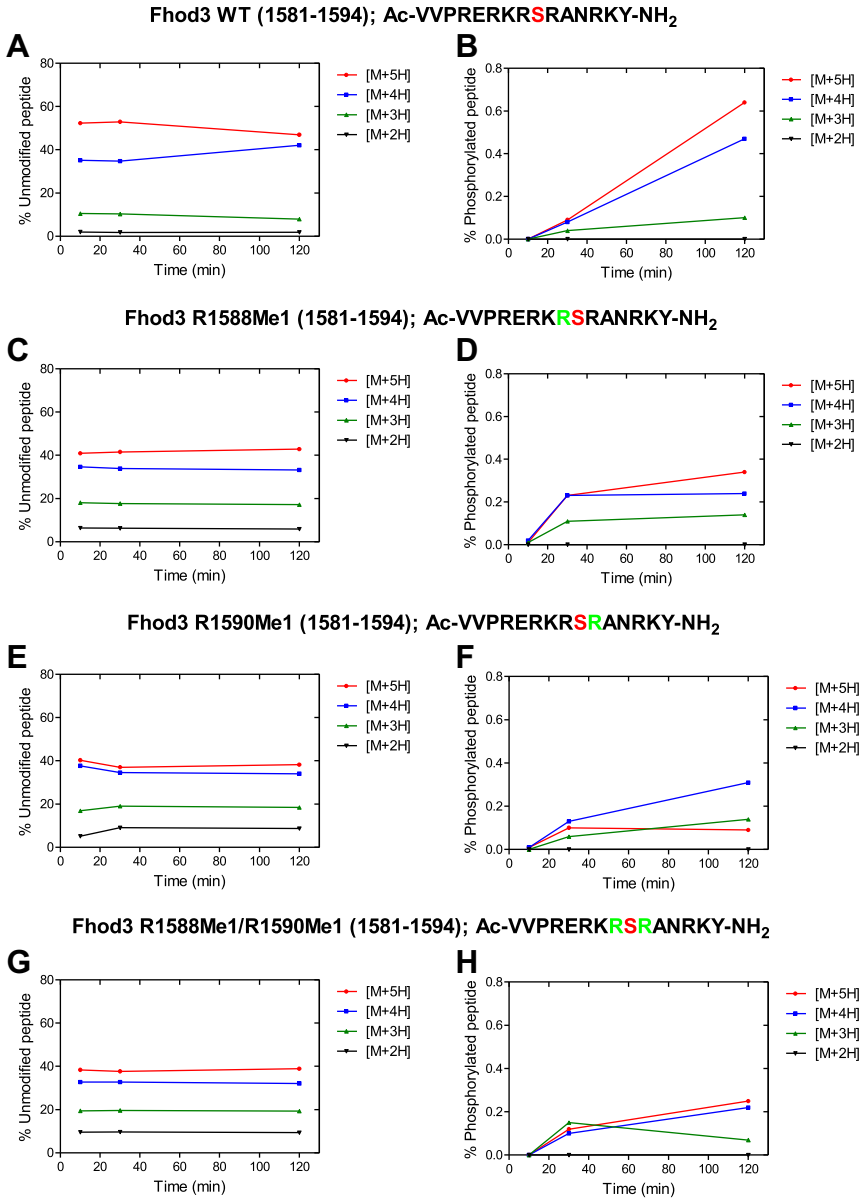

Figure 8. ROCK1 enzymatic activity is minimally affected by the presence of methylarginine residues in a peptide containing serine 1589. 130 ng of ROCK1, 1 mM ATP, and 10 μM Fhod3 (1581-1594) peptides were incubated in a water bath at 30 °C for the specified time in a final volume of 30 μl. Reactions were terminated with TFA and loaded into a vial for mass spectrometry analysis. 10 μl of the sample was injected into an Agilent QTOF 6545 with a run time of 12 min. *A* and *B*, Fhod3 WT, *C* and *D* Fhod3 R1588Me1, *E* and *F* Fhod3 R1590Me1, *G* and *H* Fhod3 R1588Me1/R1590Me1. Change in the total amount of unmodified or phosphorylated peptide in reaction mixtures from charge states [M+2H] (*black line*), [M+3H] (*green line*), [M+4H] (*blue line*), and [M+5H] (*red line*) with time.

at the RKRSR sequence at residues 1128-1132 in Fhod1 isoform 1 and 1586-1590 in Fhod3 isoform 4. This sequence is identical to the PRMT7 recognition motif of histone H2B. Despite the common sequence, we found that different arginines were preferentially methylated in histone H2B and Fhod3. Further, we noted that neither RTRSR nor RERKR sequences of Fhod3 were targets for PRMT7. Together these results suggest that additional motif elements beyond the RXR motif contribute to PRMT7 recognition and methylation. We highlight additional human proteins with the RKRSR motif in Table S1. It is noteworthy that none of these proteins have been identified as methylated species to date in proteomic studies (52).

Methylarginines are known to occur in protein domains enriched with positively charged residues and low sequence complexity as seen in intrinsically disordered regions (53). For example, the N-terminal regions of histones containing methylated arginine residues are disordered unless in contact with DNA (54). Additionally, another identified substrate for PRMT7, the Peroxisome proliferator-activated receptor gamma (PPARγ) coactivator-1 alpha (PGC-1α), is intrinsically disordered (55). Importantly the region in formins containing the methylated site can be disordered (56–58). AlphaFold structural prediction (Uniprot Q2V2M9) indicates a folded FH2 domain but not the following sequences containing the

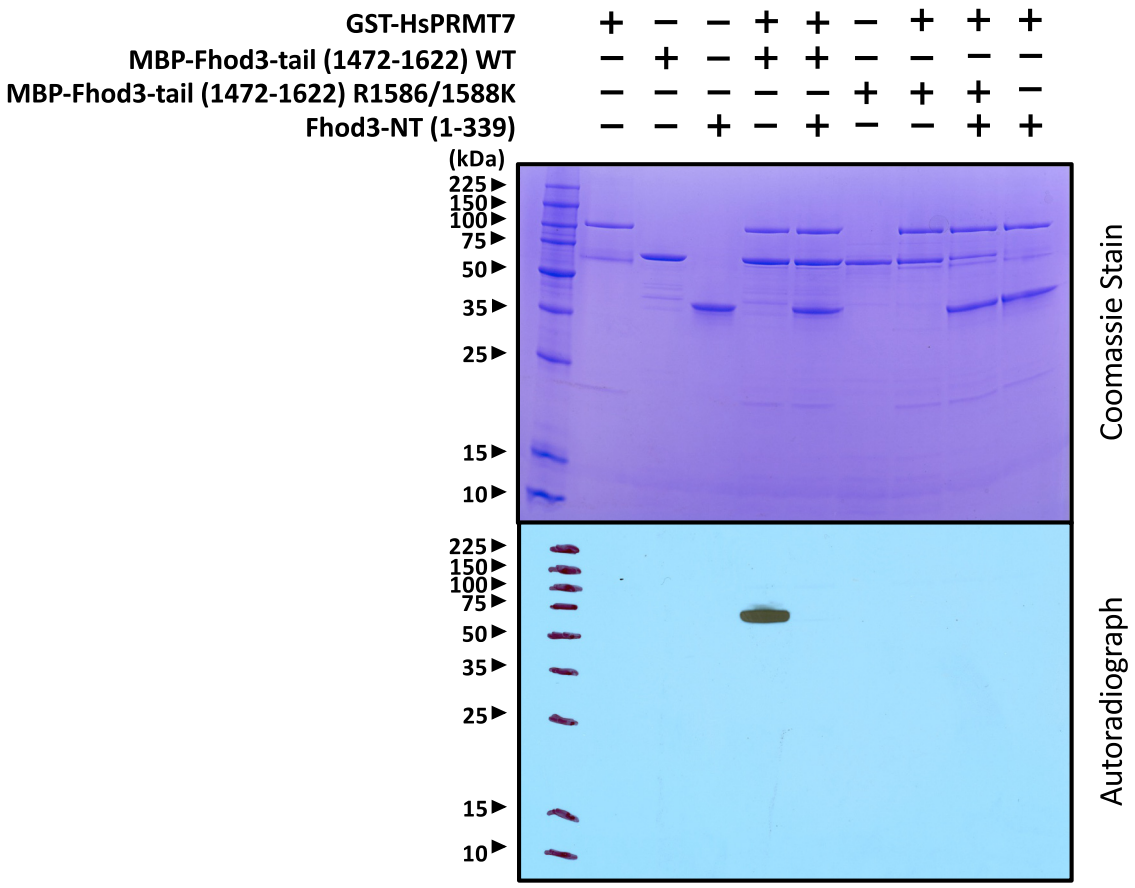

Figure 9. Methylation of Fhod3-tail by PRMT7 is abolished with the addition of the N-terminus. Radioactive gel assay of PRMT7, MBP-Fhod3-tail, and Fhod3-NT. 5 μg of GST-HsPRMT7 was mixed with 5 μg of Fhod3 NT (1-339), 5 μg MBP-Fhod3 (1472-1622) or 5 μg of MBP-Fhod3 (1472-1622) R1586/1588K. Reactions were incubated at 4 °C for 20 h in a buffer containing 50 mM K-HEPES, 1 mM DTT, and 0.7 μM [^{3}H]AdoMet in a final volume of 30 μl. Reaction mixtures were separated on an SDS-PAGE, dried, enhanced, and exposed to autoradiograph film for 30 days as described in the Experimental procedures.

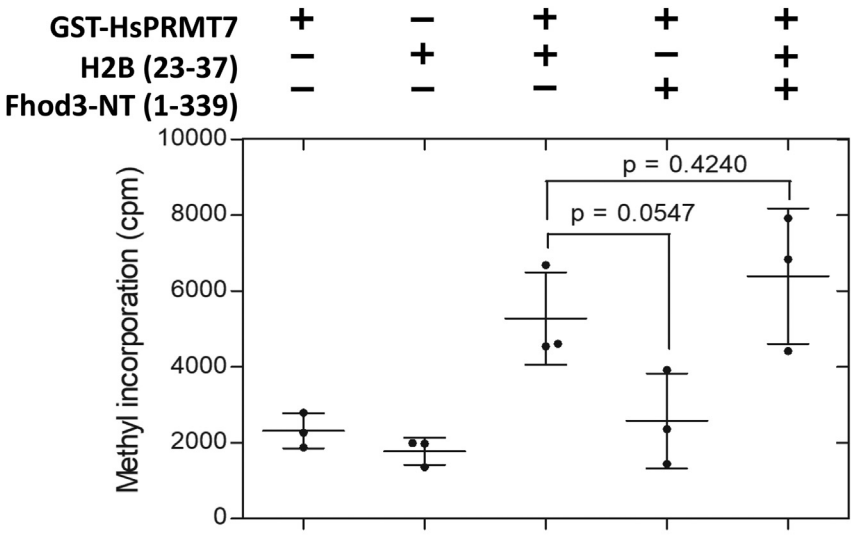

Figure 10. Methylation of H2B (23-37) peptide is not altered by the addition of Fhod3 N-terminus. P81 phosphocellulose assays of *in vitro* GST-HsPRMT7 methylation reactions with H2B (23–37) peptide as described and Fhod3-NT. 5 μg of GST-HsPRMT7 was mixed with 10 μM H2B (23–37) and/or 5 μg of Fhod3 NT (1-339). Reactions were incubated in a buffer containing 50 mM K-HEPES, 1 mM DTT, and 0.7 μM [^{3}H]AdoMet, pH 8.5 for 20 h at 4 °C in a final volume of 30 μl. Samples were terminated with 0.5 μl 100% trifluoroacetic acid and blotted on P81 phosphocellulose paper prior to liquid scintillation counting. All samples were performed in triplicate, and statistical analysis was performed using GraphPad PRISM v5.0 Students *t* test.

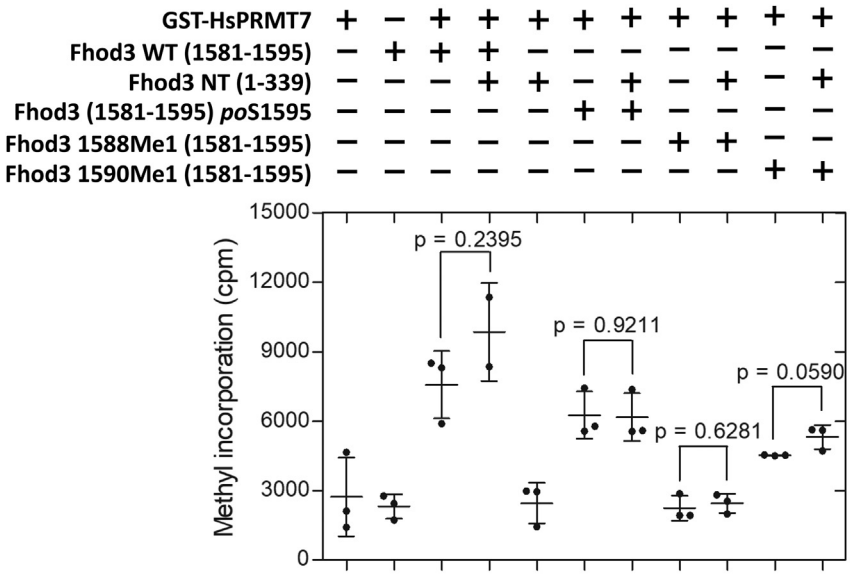

Figure 11. Methylation of Fhod3 (1581-1595) is not altered with the addition of Fhod3 N-terminus. P81 phosphocellulose assays of *in vitro* GST-HsPRMT7 methylation reactions with Fhod3 (1581-1596) peptides, as described, and Fhod3 NT. 5 μg of GST-HsPRMT7 was mixed with either 10 μM Fhod3 (1581-1595) WT, 10 μM Fhod3 (1581-1595) *po*S1595, 10 μM Fhod3 1588Me1 (1581-1595) 1588Me1, 10 μM Fhod3 1588Me1 (1581-1595) 1590Me1, and/or 5 μg of Fhod3 NT (1-339) Reactions were incubated in a buffer containing 50 mM K-HEPES, 1 mM DTT, and 0.7 μM [^{3}H]AdoMet, pH 8.5 for 20 h at 4 °C in a final volume of 30 μl. Samples were terminated with 0.5 μl 100% trifluoroacetic acid and blotted on P81 phosphocellulose paper prior to liquid scintillation counting. All samples were performed in triplicate, and statistical analysis was performed using GraphPad PRISM v5.0 Students *t* test.

RKRSR sequence, suggesting that the methylation occurs in a disordered region.

Crystal structures of the related mouse formin protein mDia1 reveal that the core C-terminal DAD domain takes on a helical fold when bound to the N-terminal DID domain but the sequence beyond this DAD domain does not appear to be ordered (59, 60). The residues beyond the DAD helix approaching the equivalent position of the RKRSR motif in Fhod1 and 3 stretches along the surface of the DID domain toward a negatively charged pocket. Unfortunately, the structure obtained from this corresponding region in mDia1 ends with only the first two residues of the basic cluster. Based on sequence alignment, the conserved RKRSR in Fhod1 and Fhod3 would follow immediately after these two ordered residues. It is noteworthy that the surface of the Fhod1 DID domain is more consistently negative than that of the mDia1 DID domain (61). Thus, the longer basic region of the Fhod formins may make additional salt bridges along the surface of the domain. Such contacts could block PRMT7 methylation in the autoinhibited state, consistent with our *in vitro* results using the N-terminal and C-terminal constructs.

The physiological role of Fhod methylation is not clear at this point. It is noteworthy that methylation is not only blocked by the interaction of the DID domain and the DAD domain but also by ROCK1 phosphorylation. Thus, it appears that methylation can be blocked in both activated and inhibited states. The question of how or whether formins are methylated *in vivo* is thus open. It is possible that Fhods may not, in fact, be substrates for PRMT7 *in vivo*. If they are, we propose two possible scenarios. First, *in vivo* regulation of Fhods may be more complex than we are aware. In fact, Fhods have conserved GTPase binding domains adjacent to their DID domains, similar to most formins. Binding of small GTPases is implicated in activation in multiple cases, but may not be sufficient for complete activation of all formins (62–64). It follows that there could be a state of Fhod formins that is not yet phosphorylated and could be methylated. Second, Fhods might be methylated co-translationally, as is the case for other proteins with arginine methyl-accepting sites (65, 66) or histidine sites (67). If this were the case, the inhibition of methylation by either the DID-DAD interaction or by phosphorylation would not be physiologically relevant. As we have demonstrated, constitutive methylation of the Fhod tails would not significantly interfere with the regulatory phosphorylation events. However, in either case, methylation could alter the binding affinity of the DID-containing N-terminus with the DAD-containing C-terminus, perhaps favoring activation for actin assembly. In addition, formin tails that include the RKRSR methylation sites make significant contributions to nucleation and elongation by binding directly to actin monomers and filaments (58, 68, 69). Interestingly, Schonichen *et al.* (2006) found that mutating this site, while not sufficient to activate Fhod1, did result in loss of localization in cells (70). Thus, further experiments are required to determine the functional impact of methylation.

Other studies have demonstrated inhibition of PRMT methylation by adjacent or nearby phosphoserine residues. In histone H3, serine-10 is known to be phosphorylated by a variety of kinases (71) and arginine-8 is methylated by PRMTs (72). However, if serine-10 is phosphorylated, then PRMT1, PRMT4, or PRMT5 catalyzed methylation of arginine-8 is completely inhibited (73). In histones H2A and H4, serine phosphorylation at positions 1 and 4 partially inhibits methylation of arginine-3 by PRMT5 (74, 75). We now extend

these observations by showing that PRMT7 methylation is inhibited by a phosphorylated serine in both Fhod3 and histone H2B. The significant inhibitory effect of phosphoserine residues on methylation of nearby arginine residues may be explained on a molecular basis by salt bridges between the positively charged and negatively charged side chains that stabilize proteins (76). Specifically, when a phosphoserine is in close proximity to arginine, the negatively charged oxygens on the phosphate group lead to non-covalent interactions with the positively charged nitrogen atoms of the arginine guanidino group (73).

Conversely, there have been two studies that demonstrate the effect of protein arginine methylation on phosphorylation. For example, methylation of arginine-1199 in the epidermal growth factor receptor stimulates the autophosphorylation of tyrosine-1197 (77). In another study, methylation of CIRBP by PRMT1 reduces the amount of phosphorylation at nearby sites by SRPK1 (78). In contrast, phosphorylation of the PRMT7 methylated site in Fhod3 was minimally impacted by methylation.

One possibility is that the inhibition of methylation by phosphorylation represents a mechanism that can be seen to parallel direct enzymatic demethylation of arginine residues. There is no clear consensus on the existence of protein arginine demethylases but JMJD6, or Jumonji domain containing 6 protein has been proposed as such an enzyme (79). JMJD6 has also been characterized as a lysine hydroxylase (80). However, MALDI-TOF experiments have shown the reduction of 14 kDa or 28 kDa of a monomethylated or dimethylated arginine peptide with the addition of the JMJD6 enzyme (81). Another proposed mechanism of arginine demethylation utilizes the protein arginine deiminase 4 enzyme, PAD4. While the function of this enzyme has been shown to catalyze citrulline from arginine, *in vitro* studies have shown that the catalysis of PAD4 on methylarginine histones resulted in methylamine formation (82). However, the rates of demodification of methylarginine by PAD4 were slower in comparison to the formation of methylarginines by PRMTs (83). Thus, inhibition of methylation may be an important way to regulate PRMTs.

While we still lack an understanding of how PRMT7 is regulated *in vivo*, our findings of the crosstalk interactions with Fhod methylation and phosphorylation do suggest possible regulatory mechanisms for formin-mediated actin polymerization. It will be intriguing to learn how the known regulation of PRMT7 by low temperature, a low ionic strength environment, and alkaline conditions (84) may contribute to the physiological process of actin polymerization.

Experimental procedures

Plasmids and constructs

The original templates, EGFP-HSFhod1 and EGFP-Fhod3L, were generously provided by T. Iskratsch (Queen Mary University of London). Human Fhod3 CT (963-1622) was cloned into a pGEX-6P-2 plasmid with a glutathione-S-transferase (GST) tag. The shorter fragments, Fhod3-tail (1472-1622) and Fhod1-tail (1110-1164) were cloned into a modified pGEX plasmid with the GST replaced by a maltose binding protein (MBP) tag. Point mutations of the MBP-Fhod3-tail (1472-1622) were generated by site-directed mutagenesis as described (85).

Human Fhod3 NT (1-339) was cloned from a pCS2+-3xHA-FHOD3 WT template into pGEX-6p-2 to provide an N-terminal GST tag, which was used for purification purposes and subsequently cleaved as described.

GST was cleaved with PreScission protease from the GST-Fhod3-CT (963-1622) and GST-Fhod3-NT (1-339) constructs prior to performing the experiments in Figures 1*C* and S9–S11. All experiments with "tail" constructs were performed on MBP-Fhod1-tail (1110-1164) or MBP-Fhod3-tail (1472-1622) wild-type or mutants without removing the tag.

Cell growth and protein purification

Recombinant *H. sapiens* GST-PRMT7 was purified as described (84). All Fhod1 and Fhod3 constructs were transformed in Rosetta 2 (DE3) cells (Novagen) and grown in 1 L of Terrific Broth supplemented with 100 mg/liter ampicillin and 32 mg/liter chloramphenicol. Expression was induced at OD 0.6 to 0.8 with 0.5 mM isopropyl-ß-D-1-thiogalactopyranoside (IPTG) and allowed to shake overnight at 18 °C, 210 rpm. Cells were harvested by centrifugation at 6000*g* for 10 min, washed in 1X phosphate buffer saline (PBS) containing 1 mM dithiothreitol (DTT), and flash frozen in liquid nitrogen.

Cell pellets expressing GST-FHOD3L-CT were resuspended in 20 mM HEPES pH 7.5, 150 mM NaCl, 1 mM PMSF, 1 mM DTT, 2 µg/ml DNaseI. All subsequent steps were performed on ice or at 4 °C. The cells were lysed by microfluidizing and cleared by centrifugation at 20,000*g* for 20 min, and then purified using a HitrapSP-FF cation exchange column (GE Life Sciences) with a gradient of 0.2 to 0.6 M NaCl over 1 column volume after 1 column volume of washing at 0.2 M NaCl. Peak fractions were dialyzed overnight into 20 mM HEPES pH 8, 200 mM NaCl, 1 mM DTT to cut off the GST with precision protease, centrifuged at 4 °C for 48,000 rpm for 20 min, and further purified on a MonoS cation exchange column (GE Life Sciences) with a gradient of 0.2 to 0.95 M NaCl over 40 column volumes after 1 column volume of washing at 0.2 M NaCl. Peak fractions were exchanged into storage buffer (10 mM Tris pH 8, 150 mM NaCl, 20% glycerol, 1 mM DTT), then flash frozen in liquid nitrogen and stored at −80 °C.

Cell pellets expressing the MBP-Fhod tails (Fhod1, Fhod3, and mutants thereof) were thawed and resuspended in 20 mM Tris, 200 mM NaCl, 1 mM EDTA, 1 mM DTT, 2 µg/ml DNaseI, 1 mM PMSF, pH 7.5. All subsequent steps were performed on ice or at 4 °C. The cells were lysed by microfluidizing and cleared by centrifugation at 20,000*g* for 20 min. Lysate was incubated with amylose resin (New England Biolabs) for 1 h at 4 °C. Resin was washed with extraction buffer (20 mM Tris, 200 mM NaCl, 1 mM EDTA, 1 mM DTT, pH

7.5). Protein was eluted using elution buffer (20 mM Tris, 200 mM NaCl, 1 mM EDTA, 1 mM DTT, 10 mM maltose), flash frozen in liquid nitrogen, and stored at −80 °C. The MBP was not removed.

Cell pellets expressing GST-Fhod3-NT (1-339) were resuspended in extraction buffer (137 mM NaCl, 2.7 mM KCl, 10 mM Na_2HPO_4, 1.8 mM KH_2PO_4, 1 mM DTT, 1 mM PMSF, 2 μg/ml DNaseI, pH 7.4). Cells were lysed by microfluidizing and cleared by centrifugation at 20,000*g* for 20 min. Clarified supernatant was incubated with glutathione Sepharose 4B resin for 1 h at 4 °C on a nutating tube rocker. The flow through was collected under gravity flow, and the resin was subsequently washed with 25 ml of extraction buffer. Fhod3-NT was eluted with 15 ml glutathione elution buffer (50 mM Tris, 150 mM NaCl, and 10 mM reduced glutathione, pH 8.0). Elution fractions were dialyzed overnight into IEC buffer A (20 mM Tris, 150 mM NaCl, 1 mM DTT at a pH of 8.0) and the GST tag was cleaved off. Cleaved and dialyzed Fhod3 NT (1-339) was then loaded onto glutathione Sepharose 4B resin and flow through was collected. The flow through was then concentrated and further purified on a MonoQ anion exchange column (GE Life Sciences). The column was washed with one column volume of IEC buffer A prior to running a 50-column volume linear gradient of IEC buffer B (20 mM Tris, 650 mM NaCl, 1 mM DTT at a pH of 8.0). Samples were exchanged into storage buffer (10 mM Tris, 150 mM NaCl, 20% glycerol, 1 mM DTT, pH = 8.0), aliquoted and flash frozen in liquid nitrogen. All samples were stored at −80 °C.

Peptide substrates

These are described in Tables 2 and 3.

Radioactive methylation assay

Gel assays of GST-HsPRMT7, MBP-Fhod1-tail (1110-1164), Fhod3-CT (963-1622), MBP-Fhod3-tail (1472-1622) wild-type and MBP-Fhod3-tail (1472-1622) arginine to lysine mutations were performed as previously described (84).

In vitro ROCK1 kinase assay

N-terminal 6xHis-tagged recombinant human ROKβ/ROCK-I (17-535) was purchased from Eurofins Discoverx (catalog No. 14-601). Kinase reactions were carried out in a reaction buffer containing 8 mM K-HEPES, 200 μM EDTA supplemented with an ATP cocktail mixture of 8 mM MgAc·6H2O and 80 μM ATP. Reactions were allowed to incubate in a 30 °C water bath for the times listed and terminated with 0.5 μl of 100% trifluoroacetic acid.

Mass spectrometry

In vitro ROCK1 kinase reactions were injected into an Agilent MS Q-TOF model G6545B with a Dual AJS ESI ion source. Scan segments were collected in positive mode with an MS absolute threshold of 200 (0.010% relative threshold), and a MS/MS absolute threshold of 5 (0.010% relative threshold). Sampler auxiliary draw speed was 200 μl/min and an eject speed of 400 μl/min. Binary pump, model G7112B, flow rate was set at 0.800 ml/min with a low-pressure limit of 0.00 bar, and a high-pressure limit of 400.0 bar. The maximum flow gradient was 100.000 ml/min^2 with a stop time of 12.0 min and a post time of 3.0 min. Mobile phase solvent A contained 0.1% FA in water and solvent B contained 0.1% FA in acetonitrile. The first 2 min contained 99% solvent A and 1% solvent B then 5% solvent A and 95% solvent B for the remainder of the run. Column composition, model G7116A, temperature was set to 40 °C. Both left and right temperature control analyses were enabled and set to 0.8 °C with an equilibration temperature time of 0.0 min. DAD, model G7115A, contained a peak width of >0.1 min (2 s response time, 2.5 Hz) with a slit of 4 nm. The analog output was offset by 5% with an attenuation of 1000 mAU and the margin for negative absorbance set to 100 mAU. The spectrum range was from 190 nm to 650 nm with a spectrum step of 2.0 nm.

P81 methylation assay

P81 assay of GST-PRMT7, phosphoserine Fhod peptides, and phosphoserine H2B peptides were performed as previously described (84).

Statistical analysis

Michaelis Menten non-linear regression was performed using GraphPad Prism version 5.01 for Windows, GraphPad Software, www.graphpad.com. No constraint was applied to the Vmax while the Km was constrained to a value greater than 0.0. No weighting method was applied and each replicate Y value was considered as an individual point.

Student *t* test was performed using GraphPad Prism version 5.01 for Windows, GraphPad Software, San Diego California USA, www.graphpad.com.

Table 2
Arginine methylation P81 peptides

Peptide name	Peptide sequence	Purity (%)	Theoretical MW
H2B (23-37) WT	Ac-KKDGKKRKRSRKESY-NH_2	87.8	1935.25
H2B (23-37) *po*S32	KKDGKKRKR{*po*SER}RKESY	91.0	1974.18
H2B (23-37) *po*S36	KKDGKKRKRSRKE{*po*SER}Y	88.3	1974.18
Fhod3 (1581-1595) WT	VVPRERKRSRANRKSY	98.2	2002.3
Fhod3 (1581-1595) *po*S1589	VVPRERKR{*po*SER}RANRKSY	87.2	2082.28
Fhod3 (1581-1595) *po*S1595	VVPRERKRSRANRK{*po*SER}Y	96.9	2082.28

All peptides were purchased from GenScript. Trifluoroacetic acid removal was performed by company and switched with a standard acetate salt. A tyrosine residue was added at the C-terminus of each Fhod peptide to determine the concentration of the peptide by UV spectra.

Table 3
Serine phosphorylation mass spectrometry peptides

Peptide name	Peptide sequence	Purity (%)	Theoretical MW
Fhod3 (1581-1594) WT	Ac-VVPRERKRSRANRKY-NH_2	88.4	1956.33
Fhod3 (1581-1594) R1588Me1	Ac-VVPRERK{RMe1}SRANRKY-NH_2	87.2	1970.33
Fhod3 (1581-1594) R1590Me1	Ac-VVPRERKRS{RMe1}ANRKY-NH_2	96.9	1970.33
Fhod3 (1581-1594) R1588Me1/R1590Me1	Ac-VVPRERK{RMe1}S{RMe1}ANRKY-NH_2	99.1	1984.38
Fhod3 (1581-1595) WT	Ac-VVPRERKRSRANRKSY-NH_2	97.6	2043.35
Fhod3 (1581-1595) R1588Me1	Ac-VVPRERK{RMe1}SRANRKSY-NH_2	97.6	2057.40
Fhod3 (1581-1595) R1590Me1	Ac-VVPRERKRS{RMe1}ANRKSY-NH_2	99.1	2057.40
Fhod3 (1581-1595) R1588Me1/R1590Me1	Ac-VVPRERK{RMe1}S{RMe1}ANRKSY-NH_2	94.1	2071.46

All peptides were purchased from GenScript. Trifluoroacetic acid removal was performed by company and switched with a standard acetate salt. A tyrosine residue was added at the C-terminus of each Fhod peptide to determine the concentration of the peptide by UV spectra.

Data availability

All mass spectrometry raw files have been deposited in the MassIVE repository housed at UCSD (http://massive.ucsd.edu/) with the accession number MSV000094470 [https://doi.org/10.25345/C5T14V12K]. FTP files can be directly downloaded from [ftp://massive.ucsd.edu/v07/MSV000094470/]. Additional data are available upon request.

Supporting information—This article contains supporting information.

Author contributions—T. L. L., S. G. C., M. E. Q., V. E. V., and D. A. V. writing–review & editing; T. L. L. writing–original draft; T. L. L., S. G. C., M. E. Q., and D. A. V. visualization; T. L. L., S. G. C., M. E. Q., and D. A. V. validation; T. L. L., V. E. V., and D. A. V. resources; T. L. L., S. G. C., and M. E. Q. methodology; T. L. L., V. E. V., and D. A. V. investigation; T. L. L. and S. G. C. formal analysis; T. L. L. and S. G. C. data curation; T. L. L., S. G. C., M. E. Q., and D. A. V. conceptualization; S. G. C. and M. E. Q. supervision; T. L. L., S. G. C., M. E. Q., and D. A. V. project administration; S. G. C. and M. E. Q. funding acquisition.

Funding and additional information—This work was supported by the National Science Foundation grant MCB-1714569 (to S. G. C.). The work was also supported by National Institutes of Health grant R01HL146159 (to M. E. Q.). T. L. and D. A. V. were supported by the National Institutes of Health Ruth L. Kirschstein National Research Service Award GM007185.

Conflict of interests—The authors declare that they have no conflicts of interest with the contents of this article.

Abbreviations—The abbreviations used are: DAD, diaphanous autoinhibitory domain; Fhods, Formin Homology Domain-containing proteins; PRMT7, protein arginine methyltransferase 7; PTM, post-translational modifications; TAFs, TBP-associated factors; TBP, TATA-binding proteins.

References

1. Hampsey, M., and Reinberg, D. (1997) Transcription: why are TAFs essential? *Curr. Biol.* **7**, R44–R46
2. Whitmarsh, A. J., and Davis, R. J. (2000) Regulation of transcription factor function by phosphorylation. *Cell Mol. Life Sci.* **57**, 1172–1183
3. Choudhary, C., Kumar, C., Gnad, F., Nielsen, M. L., Rehman, M., Walther, T. C., *et al.* (2009) Lysine acetylation targets protein complexes and co-regulates major cellular functions. *Science* **325**, 834–840
4. Guo, A., Gu, H., Zhou, J., Mulhern, D., Wang, Y., Lee, K. A., *et al.* (2014) Immunoaffinity enrichment and mass spectrometry analysis of protein methylation. *Mol. Cell Proteomics* **13**, 372–387
5. Pham, H. Q. H., Tao, X., and Yang, Y. (2023) Protein arginine methylation in transcription and epigenetic regulation. *Front. Epigenet. Epigenom.* https://doi.org/10.3389/freae.2023.1245832
6. Fuhrmann, J., Clancy, K. W., and Thompson, P. R. (2015) Chemical biology of protein arginine modifications in epigenetic regulation. *Chem. Rev.* **115**, 5413–5461
7. Bedford, M. T., and Clarke, S. G. (2009) Protein arginine methylation in mammals: who, what, and why. *Mol. Cell* **33**, 1–13
8. Horowitz, S., and Trievel, R. C. (2012) Carbon-oxygen hydrogen bonding in biological structure and function. *J. Biol. Chem.* **287**, 41576–41582
9. Evich, M., Stroeva, E., Zheng, Y. G., and Germann, M. W. (2016) Effect of methylation on the side-chain pKa value of arginine. *Protein Sci.* **25**, 479–486
10. Eram, M. S., Shen, Y., Szewczyk, M., Wu, H., Senisterra, G., Li, F., *et al.* (2016) A potent, selective and cell-active inhibitor of human type I protein arginine methyltransferases. *ACS Chem. Biol.* **11**, 772–781
11. Fulton, M. D., Brown, T., and Zheng, Y. G. (2018) Mechanisms and inhibitors of histone arginine methylation. *Chem. Rec.* **18**, 1792–1807
12. Zurita-Lopez, C. I., Sandberg, T., Kelly, R., and Clarke, S. G. (2012) Human protein arginine methyltransferase 7 (PRMT7) is a type III enzyme forming ω-NG-monomethylated arginine residues. *J. Biol. Chem.* **287**, 7859–7870
13. Bondoc, T. J., Lowe, T. L., and Clarke, S. G. (2023) The exquisite specificity of human protein arginine methyltransferase 7 (PRMT7) toward Arg-X-Arg sites. *PLoS One* **18**, e0285812
14. Feng, Y., Maity, R., Whitelegge, J. P., Hadjikyriacou, A., Li, Z., Zurita-Lopez, C., *et al.* (2013) Mammalian protein arginine methyltransferase 7 (PRMT7) specifically targets RXR sites in lysine- and arginine-rich regions. *J. Biol. Chem.* **288**, 37010–37025
15. Bhullar, K. S., Lagarón, N. O., McGowan, E. M., Parmar, I., Jha, A., Hubbard, B. P., *et al.* (2018) Kinase-targeted cancer therapies: progress, challenges and future directions. *Mol. Cancer* **17**, 48
16. McKenna, M., Balasuriya, N., Zhong, S., Li, S. S.-C., and O'Donoghue, P. (2020) Phospho-form specific substrates of protein kinase B (AKT1). *Front. Bioeng. Biotechnol.* **8**, 619252
17. Separovich, R. J., Wong, M. W. M., Chapman, T. R., Slavich, E., Hamey, J. J., and Wilkins, M. R. (2021) Post-translational modification analysis of Saccharomyces cerevisiae histone methylation enzymes reveals phosphorylation sites of regulatory potential. *J. Biol. Chem.* **296**, 100192
18. Yao, R., Jiang, H., Ma, Y., Wang, L., Wang, L., Du, J., *et al.* (2014) PRMT7 induces epithelial-to-mesenchymal transition and promotes metastasis in breast cancer. *Cancer Res.* **74**, 5656–5667
19. Günes Günsel, G., Conlon, T. M., Jeridi, A., Kim, R., Ertüz, Z., Lang, N. J., *et al.* (2022) The arginine methyltransferase PRMT7 promotes extravasation of monocytes resulting in tissue injury in COPD. *Nat. Commun.* **13**, 1303
20. Wang, B., Zhang, M., Liu, Z., Mu, Y., and Li, K. (2021) PRMT7: a pivotal arginine methyltransferase in stem cells and development. *Stem Cells Int.* **2021**, 6241600
21. Agolini, E., Dentici, M. L., Bellacchio, E., Alesi, V., Radio, F. C., Torella, A., *et al.* (2018) Expanding the clinical and molecular spectrum of

PRMT7 mutations: 3 additional patients and review. *Clin. Genet.* **93**, 675–681
22. Cali, E., Suri, M., Scala, M., Ferla, M. P., Alavi, S., Faqeih, E. A., *et al.* (2023) Biallelic PRMT7 pathogenic variants are associated with a recognizable syndromic neurodevelopmental disorder with short stature, obesity, and craniofacial and digital abnormalities. *Genet. Med.* **25**, 135–142
23. Poquérusse, J., Whitford, W., Taylor, J., Alburaiky, S., Snell, R. G., Lehnert, K., *et al.* (2022) Novel PRMT7 mutation in a rare case of dysmorphism and intellectual disability. *J. Hum. Genet.* **67**, 19–26
24. So, H.-K., Kim, S., Kang, J.-S., and Lee, S.-J. (2021) Role of protein arginine methyltransferases and inflammation in muscle pathophysiology. *Front. Physiol.* **12**, 712389
25. Jeong, H.-J., Lee, H.-J., Vuong, T. A., Choi, K.-S., Choi, D., Koo, S.-H., *et al.* (2016) Prmt7 deficiency causes reduced skeletal muscle oxidative metabolism and age-related obesity. *Diabetes* **65**, 1868–1882
26. Blanc, R. S., Vogel, G., Chen, T., Crist, C., and Richard, S. (2016) PRMT7 preserves satellite cell regenerative capacity. *Cell Rep.* **14**, 1528–1539
27. Rohn, J. L., and Baum, B. (2010) Actin and cellular architecture at a glance. *J. Cell Sci.* **123**, 155–158
28. Valencia, D. A., and Quinlan, M. E. (2021) Formins. *Curr. Biol.* **31**, R517–R522
29. Labat-de-Hoz, L., and Alonso, M. A. (2021) Formins in human disease. *Cells* **10**, 2554
30. Shimada, A., Nyitrai, M., Vetter, I. R., Kühlmann, D., Bugyi, B., Narumiya, S., *et al.* (2004) The core FH2 domain of diaphanous-related formins is an elongated actin binding protein that inhibits polymerization. *Mol. Cell* **13**, 511–522
31. Xu, Y., Moseley, J. B., Sagot, I., Poy, F., Pellman, D., Goode, B. L., *et al.* (2004) Crystal structures of a Formin Homology-2 domain reveal a tethered dimer architecture. *Cell* **116**, 711–723
32. Tojo, H., Kaieda, I., Hattori, H., Katayama, N., Yoshimura, K., Kakimoto, S., *et al.* (2003) The Formin family protein, formin homolog overexpressed in spleen, interacts with the insulin-responsive aminopeptidase and profilin IIa. *Mol. Endocrinol.* **17**, 1216–1229
33. Dwyer, J., Pluess, M., Iskratsch, T., Dos Remedios, C. G., and Ehler, E. (2014) The formin FHOD1 in cardiomyocytes. *Anat. Rec. (Hoboken)* **297**, 1560–1570
34. Schönichen, A., Mannherz, H. G., Behrmann, E., Mazur, A. J., Kühn, S., Silván, U., *et al.* (2013) FHOD1 is a combined actin filament capping and bundling factor that selectively associates with actin arcs and stress fibers. *J. Cell Sci.* **126**, 1891–1901
35. Kutscheidt, S., Zhu, R., Antoku, S., Luxton, G. W. G., Stagljar, I., Fackler, O. T., *et al.* (2014) FHOD1 interaction with nesprin-2G mediates TAN line formation and nuclear movement. *Nat. Cell Biol.* **16**, 708–715
36. Gardberg, M., Kaipio, K., Lehtinen, L., Mikkonen, P., Heuser, V. D., Talvinen, K., *et al.* (2013) FHOD1, a formin upregulated in epithelial-mesenchymal transition, participates in cancer cell migration and invasion. *PLoS One* **8**, e74923
37. Antoku, S., Schwartz, T. U., and Gundersen, G. G. (2023) FHODs: nuclear tethered formins for nuclear mechanotransduction. *Front. Cell Dev. Biol.* **11**, 1160219
38. Ushijima, T., Fujimoto, N., Matsuyama, S., Kan-O, M., Kiyonari, H., Shioi, G., *et al.* (2018) The actin-organizing formin protein Fhod3 is required for postnatal development and functional maintenance of the adult heart in mice. *J. Biol. Chem.* **293**, 148–162
39. Taniguchi, K., Takeya, R., Suetsugu, S., Kan-O, M., Narusawa, M., Shiose, A., *et al.* (2009) Mammalian formin fhod3 regulates actin assembly and sarcomere organization in striated muscles. *J. Biol. Chem.* **284**, 29873–29881
40. Walsh, R., Offerhaus, J. A., Tadros, R., and Bezzina, C. R. (2022) Minor hypertrophic cardiomyopathy genes, major insights into the genetics of cardiomyopathies. *Nat. Rev. Cardiol.* **19**, 151–167
41. vanLieshout, T. L., and Ljubicic, V. (2019) The emergence of protein arginine methyltransferases in skeletal muscle and metabolic disease. *Am. J. Physiol. Endocrinol. Metab.* **317**, E1070–E1080
42. Herrmann, F., Pably, P., Eckerich, C., Bedford, M. T., and Fackelmayer, F. O. (2009) Human protein arginine methyltransferases in vivo–distinct properties of eight canonical members of the PRMT family. *J. Cell Sci.* **122**, 667–677
43. Haghandish, N., Baldwin, R. M., Morettin, A., Dawit, H. T., Adhikary, H., Masson, J.-Y., *et al.* (2019) PRMT7 methylates eukaryotic translation initiation factor 2α and regulates its role in stress granule formation. *Mol. Biol. Cell* **30**, 778–793
44. Zhou, Q., Wei, S.-S., Wang, H., Wang, Q., Li, W., Li, G., *et al.* (2017) Crucial role of ROCK2-mediated phosphorylation and upregulation of FHOD3 in the pathogenesis of angiotensin II-induced cardiac hypertrophy. *Hypertension* **69**, 1070–1083
45. Iskratsch, T., Reijntjes, S., Dwyer, J., Toselli, P., Dégano, I. R., Dominguez, I., *et al.* (2013) Two distinct phosphorylation events govern the function of muscle FHOD3. *Cell Mol. Life Sci.* **70**, 893–908
46. Parra, M. A., Kerr, D., Fahy, D., Pouchnik, D. J., and Wyrick, J. J. (2006) Deciphering the roles of the histone H2B N-terminal domain in genome-wide transcription. *Mol. Cell Biol.* **26**, 3842–3852
47. Mao, P., Kyriss, M. N. M., Hodges, A. J., Duan, M., Morris, R. T., Lavine, M. D., *et al.* (2016) A basic domain in the histone H2B N-terminal tail is important for nucleosome assembly by FACT. *Nucleic Acids Res.* **44**, 9142
48. Lau, A. T. Y., Lee, S.-Y., Xu, Y.-M., Zheng, D., Cho, Y.-Y., Zhu, F., *et al.* (2011) Phosphorylation of histone H2B serine 32 is linked to cell transformation. *J. Biol. Chem.* **286**, 26628–26637
49. Monteonofrio, L., Valente, D., Ferrara, M., Camerini, S., Miscione, R., Crescenzi, M., *et al.* (2018) HIPK2 and extrachromosomal histone H2B are separately recruited by Aurora-B for cytokinesis. *Oncogene* **37**, 3562–3574
50. Yi, S. A., Um, S. H., Lee, J., Yoo, J. H., Bang, S. Y., Park, E. K., *et al.* (2016) S6K1 phosphorylation of H2B mediates EZH2 trimethylation of H3: a determinant of Early adipogenesis. *Mol. Cell* **62**, 443–452
51. Bungard, D., Fuerth, B. J., Zeng, P.-Y., Faubert, B., Maas, N. L., Viollet, B., *et al.* (2010) Signaling kinase AMPK activates stress-promoted transcription *via* histone H2B phosphorylation. *Science* **329**, 1201–1205
52. Szewczyk, M. M., Ishikawa, Y., Organ, S., Sakai, N., Li, F., Halabelian, L., *et al.* (2020) Pharmacological inhibition of PRMT7 links arginine monomethylation to the cellular stress response. *Nat. Commun.* **11**, 2396
53. Lorton, B. M., and Shechter, D. (2019) Cellular consequences of arginine methylation. *Cell Mol. Life Sci.* **76**, 2933–2956
54. Luger, K., and Richmond, T. J. (1998) The histone tails of the nucleosome. *Curr. Opin. Genet. Dev.* **8**, 140–146
55. Mendoza, M., Mendoza, M., Lubrino, T., Briski, S., Osuji, I., Cuala, J., *et al.* (2023) Arginine methylation of the PGC-1α C-terminus is temperature-dependent. *Biochemistry* **62**, 22–34
56. Vizcarra, C. L., Kreutz, B., Rodal, A. A., Toms, A. V., Lu, J., Zheng, W., *et al.* (2011) Structure and function of the interacting domains of Spire and Fmn-family formins. *Proc. Natl. Acad. Sci. U. S. A.* **108**, 11884–11889
57. Silkworth, W. T., Kunes, K. L., Nickel, G. C., Phillips, M. L., Quinlan, M. E., and Vizcarra, C. L. (2018) The neuron-specific formin Delphilin nucleates nonmuscle actin but does not enhance elongation. *Mol. Biol. Cell* **29**, 610–621
58. Bremer, K. V., Wu, C., Patel, A. A., He, K. L., Grunfeld, A. M., Chanfreau, G. F., *et al.* (2024) Formin tails act as a switch, inhibiting or enhancing processive actin elongation. *J. Biol. Chem.* **300**, 105557
59. Nezami, A., Poy, F., Toms, A., Zheng, W., and Eck, M. J. (2010) Crystal structure of a complex between amino and carboxy terminal fragments of mDia1: insights into autoinhibition of diaphanous-related formins. *PLoS One* **5**, e12992
60. Otomo, T., Tomchick, D. R., Otomo, C., Machius, M., and Rosen, M. K. (2010) Crystal structure of the Formin mDia1 in autoinhibited conformation. *PLoS One* **5**, e12896
61. Schulte, A., Stolp, B., Schönichen, A., Pylypenko, O., Rak, A., Fackler, O. T., *et al.* (2008) The human formin FHOD1 contains a bipartite structure of FH3 and GTPase-binding domains required for activation. *Structure* **16**, 1313–1323
62. Li, F., and Higgs, H. N. (2005) Dissecting requirements for auto-inhibition of actin nucleation by the formin, mDia1. *J. Biol. Chem.* **280**, 6986–6992
63. Rose, R., Weyand, M., Lammers, M., Ishizaki, T., Ahmadian, M. R., and Wittinghofer, A. (2005) Structural and mechanistic insights into the interaction between Rho and mammalian Dia. *Nature* **435**, 513–518

64. Lammers, M., Rose, R., Scrima, A., and Wittinghofer, A. (2005) The regulation of mDia1 by autoinhibition and its release by Rho*GTP. *EMBO J.* **24**, 4176–4187
65. Wang, C., Lazarides, E., O'Connor, C. M., and Clarke, S. (1982) Methylation of chicken fibroblast heat shock proteins at lysyl and arginyl residues. *J. Biol. Chem.* **257**, 8356–8362
66. Najbauer, J., Johnson, B. A., and Aswad, D. W. (1992) Analysis of stable protein methylation in cultured cells. *Arch. Biochem. Biophys.* **293**, 85–92
67. Wilkinson, A. W., Diep, J., Dai, S., Liu, S., Ooi, Y. S., Song, D., *et al.* (2019) SETD3 is an actin histidine methyltransferase that prevents primary dystocia. *Nature* **565**, 372–376
68. Gould, C. J., Maiti, S., Michelot, A., Graziano, B. R., Blanchoin, L., and Goode, B. L. (2011) The formin DAD domain plays dual roles in autoinhibition and actin nucleation. *Curr. Biol.* **21**, 384–390
69. Vizcarra, C. L., Bor, B., and Quinlan, M. E. (2014) The role of formin tails in actin nucleation, processive elongation, and filament bundling. *J. Biol. Chem.* **289**, 30602–30613
70. Schönichen, A., Alexander, M., Gasteier, J. E., Cuesta, F. E., Fackler, O. T., and Geyer, M. (2006) Biochemical characterization of the diaphanous autoregulatory interaction in the formin homology protein FHOD1. *J. Biol. Chem.* **281**, 5084–5093
71. Komar, D., and Juszczynski, P. (2020) Rebelled epigenome: histone H3S10 phosphorylation and H3S10 kinases in cancer biology and therapy. *Clin. Epigenet.* **12**, 147
72. Di Lorenzo, A., and Bedford, M. T. (2011) Histone arginine methylation. *FEBS Lett.* **585**, 2024–2031
73. Leal, J. A., Estrada-Tobar, Z. M., Wade, F., Mendiola, A. J. P., Meza, A., Mendoza, M., *et al.* (2021) Phosphoserine inhibits neighboring arginine methylation in the RKS motif of histone H3. *Arch. Biochem. Biophys.* **698**, 108716
74. Ho, M.-C., Wilczek, C., Bonanno, J. B., Xing, L., Seznec, J., Matsui, T., *et al.* (2013) Structure of the arginine methyltransferase PRMT5-MEP50 reveals a mechanism for substrate specificity. *PLoS One* **8**, e57008f
75. Fulton, M. D., Dang, T., Brown, T., and Zheng, Y. G. (2022) Effects of substrate modifications on the arginine dimethylation activities of PRMT1 and PRMT5. *Epigenetics* **17**, 1–18
76. Horovitz, A., Serrano, L., Avron, B., Bycroft, M., and Fersht, A. R. (1990) Strength and co-operativity of contributions of surface salt bridges to protein stability. *J. Mol. Biol.* **216**, 1031–1044
77. Hsu, J.-M., Chen, C.-T., Chou, C.-K., Kuo, H.-P., Li, L.-Y., Lin, C.-Y., *et al.* (2011) Crosstalk between Arg 1175 methylation and Tyr 1173 phosphorylation negatively modulates EGFR-mediated ERK activation. *Nat. Cell Biol.* **13**, 174–181
78. Lenard, A. J., Hutten, S., Zhou, Q., Usluer, S., Zhang, F., Bourgeois, B. M. R., *et al.* (2021) Phosphorylation regulates CIRBP arginine methylation, transportin-1 binding and liquid-liquid phase separation. *Front. Mol. Biosci.* **8**, 689687
79. Chang, B., Chen, Y., Zhao, Y., and Bruick, R. K. (2007) JMJD6 is a histone arginine demethylase. *Science* **318**, 444–447
80. Poulard, C., Corbo, L., and Le Romancer, M. (2016) Protein arginine methylation/demethylation and cancer. *Oncotarget* **7**, 67532–67550
81. Liu, W., Ma, Q., Wong, K., Li, W., Ohgi, K., Zhang, J., *et al.* (2013) Brd4 and JMJD6-associated anti-pause enhancers in regulation of transcriptional pause release. *Cell* **155**, 1581–1595
82. Wang, Y., Wysocka, J., Sayegh, J., Lee, Y.-H., Perlin, J. R., Leonelli, L., *et al.* (2004) Human PAD4 regulates histone arginine methylation levels via demethylimination. *Science* **306**, 279–283
83. Thompson, P. R., and Fast, W. (2006) Histone citrullination by protein arginine deiminase: is arginine methylation a green light or a roadblock? *ACS Chem. Biol.* **1**, 433–441
84. Lowe, T. L., and Clarke, S. G. (2022) Human protein arginine methyltransferases (PRMTs) can be optimally active under nonphysiological conditions. *J. Biol. Chem.* **298**, 102290
85. Liu, H., and Naismith, J. H. (2008) An efficient one-step site-directed deletion, insertion, single and multiple-site plasmid mutagenesis protocol. *BMC Biotechnol.* **8**, 91